"Stapler" mechanism for a dipole band in ^{79}Se

C. G. Li (李晨光),[1,2] Q. B. Chen (陈启博),[1,3] S. Q. Zhang (张双全),[1,*] C. Xu (徐川),[1] H. Hua (华辉),[1,†]
S. Y. Wang (王守宇),[4] R. A. Bark,[5] S. M. Wyngaardt,[6] Z. Shi (施智),[7] A. C. Dai (戴阿灿),[1] C. G. Wang (王春光),[1]
X. Q. Li (李湘庆),[1] Z. H. Li (李智焕),[1] J. Meng (孟杰),[1,7,8] F. R. Xu (许甫荣),[1] Y. L. Ye (叶沿林),[1] D. X. Jiang (江栋兴),[1]
R. Han (韩蕊),[1] C. Y. Niu (牛晨阳),[1] Z. Q. Chen (陈志强),[1] H. Y. Wu (吴鸿毅),[1] X. Wang (王翔),[1] D. W. Luo (罗迪雯),[1]
C. G. Wu (武晨光),[1] S. Wang (王硕),[4] D. P. Sun (孙大鹏),[4] C. Liu (刘晨),[4] Z. Q. Li (李志泉),[4] B. H. Sun (孙保华),[7]
P. Jones,[5] L. Msebi,[5,9] J. F. Sharpey-Schafer,[9] T. Dinoko,[5,9] E. A. Lawrie,[5,9] S. S. Ntshangase,[10] B. V. Kheswa,[5,6]
O. Shirinda,[5,6] N. Khumalo,[5,9] T. D. Bucher,[5,6] and K. L. Malatji[5,6]

[1]*School of Physics and State Key Laboratory of Nuclear Physics and Technology, Peking University, Beijing 100871, China*
[2]*Institute of Materials, China Academy of Engineering Physics, Jiangyou 621908, China*
[3]*Physik-Department, Technische Universität München, D-85747 Garching, Germany*
[4]*Shandong Provincial Key Laboratory of Optical Astronomy and Solar-Terrestrial Environment,*
Institute of Space Sciences, Shandong University, Weihai 264209, China
[5]*iThemba LABS, 7129 Somerset West, South Africa*
[6]*Department of Physics, University of Stellenbosch, Matieland 7602, South Africa*
[7]*School of Physics and Nuclear Energy Engineering, Beihang University, Beijing 100191, China*
[8]*Yukawa Institute for Theoretical Physics, Kyoto University, Kyoto 606-8502, Japan*
[9]*Department of Physics, University of the Western Cape, P/B X17 Bellville 7535, South Africa*
[10]*Department of Physics, University of Zululand, Private Bag X1001, KwaDlangezwa 3886, South Africa*

The spectroscopy of ^{79}Se is studied via the ^{82}Se$(\alpha, \alpha 3n)^{79}$Se fusion-evaporation reaction. A negative-parity magnetic dipole band in ^{79}Se is established for the first time. Based on the calculations by the self-consistent tilted axis cranking covariant density functional theory, this new dipole band can be classified as a "stapler" band, which has a relatively stable symmetric prolate deformation as a function of rotational frequency. Hence, it is demonstrated that the stapler bands exist not only in the oblate and triaxial nuclei, but also in prolate nuclei. By examining the angular momentum coupling, it is found that the five valence nucleons in the high-j orbitals play a major role in the closing of the stapler.

I. INTRODUCTION

Nuclear collective rotation, which involves coherent contributions from many nucleons, has been well known for a long time [1,2]. It is ascribed as a consequence of deformation [3] and gives rise to regular rotational bands, which are characterized by strong electric quadrupole ($E2$) transitions. Studies of the rotational bands in nuclei have been in the forefront of nuclear structure physics and have led to many interesting phenomena including the backbending [4], superdeformed bands [5], and chiral doublet bands [6–8].

In the past two decades, a new type of rotational-like sequences, which have strong $M1$ transitions and weak or vanishing $E2$ transitions, has been discovered in weakly deformed or near-spherical nuclei [9,10] and has attracted a lot of interest [11–14]. It cannot be understood in terms of the conventional rotation of deformed nuclei but has been successfully interpreted in terms of the shears mechanism [15].

In this mechanism, the proton and neutron angular momenta are almost perpendicular to each other at the bandhead. Along the band, the excitation energy and angular momentum are increased mainly by the gradual alignments of the proton and neutron angular momenta along the total angular momentum, and consequently the orientation of the total angular momentum in the intrinsic frame remains approximately constant. This process looks like the closing of a pair of shear blades. In contrast with the conventional collective rotation (called "electric rotation") in well-deformed nuclei, this new type of rotation is called "magnetic rotation" [9].

The magnetic rotation and electric rotation represent two extreme cases that can be well distinguished. Recently an angular momentum generating mechanism called "stapler" mechanism, which is a variant of the shears mechanism, was proposed for ^{115}In [16] and ^{75}As [17] based on the angular momentum analyses by the tilted axis cranking covariant density functional theory (TAC-CDFT) [14]. In the stapler mechanism, only the neutron (proton) angular momentum moves obviously toward the direction of the total angular momentum while the proton (neutron) angular momentum is almost motionless. As a result, the tilted angle of the total
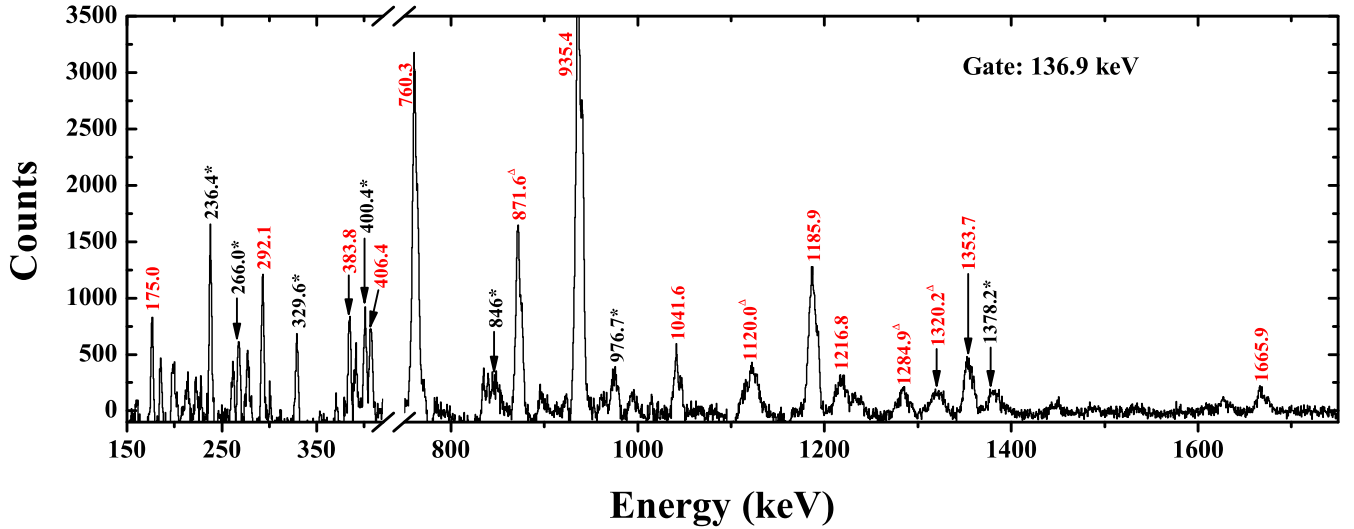
*sqzhang@pku.edu.cn
†hhua@pku.edu.cn

FIG. 1. Coincident γ-ray spectrum with gating on the 136.9-keV transition. For visual convenience, transitions of ^{79}Se are marked in red. The peaks marked with triangles belong to ^{79}Se but are not included in the partial level scheme of Fig. 3 and the peaks marked with stars are known contaminants from other nuclei.

angular momentum has an obvious change. This feature is more like the closing of a stapler; thus the observed magnetic dipole band was named as "stapler band". For the stapler band in ^{115}In, the electric rotation of a nearly oblate core was found to play a more dominant role than the magnetic rotation [16], whereas for the one in ^{75}As, the valence nucleons in high-j orbitals rather than the core are responsible for the closing of the stapler of angular momentum [17].

So far, only four stapler bands have been suggested, in ^{57}Mn [18], ^{75}As [17], ^{115}In [16], and ^{144}Tb [19]. It is worthwhile to explore more examples of stapler bands in different mass regions and to better understand the interplay between the magnetic rotation and electric rotation. Here we report on a spectroscopic study of ^{79}Se through the ^{82}Se(α, $\alpha 3n$)^{79}Se fusion-evaporation reaction. The previously established positive-parity band in ^{79}Se is confirmed in the present work and a new negative-parity stapler band is reported. With the new results in ^{79}Se and the comparison with the earlier reported stapler band in ^{75}As, the stapler mechanism in the $A \approx 80$ mass region is investigated using TAC-CDFT.

II. EXPERIMENT

The present experiment was performed at iThemba LABS in South Africa. Excited states of ^{79}Se were populated via the ^{82}Se(α, $\alpha 3n$)^{79}Se fusion-evaporation reaction at beam energies of 65 and 68 MeV. The ^{82}Se target with a thickness of 0.36 mg/cm^2 on 0.01 mg/cm^2 ^{12}C backing was used. The de-excitation γ-rays were detected by the AFRODITE [20] array, which consisted of eight Compton-suppressed clover detectors at the time of the experiment. The clover detectors were arranged in two rings at 90° (four clovers) and 135° (four clovers) with respect to the beam direction.

A total of 1.45×10^9 coincident events were collected, from which a symmetric γ–γ matrix was built. The level scheme analysis was performed using the RADWARE software [21]. The typical γ-ray spectrum gated on the 136.9-keV

γ-ray transition in ^{79}Se is shown in Fig. 1. To better show the γ-ray transitions of ^{79}Se in the spectrum, the energy region 420–750 keV, where no γ transitions of ^{79}Se were observed, is cut. In order to obtain the directional correlations of γ rays de-exciting oriented states (DCO) intensity ratios to determine the multipolarities of γ-ray transitions, the detectors around 90° with respect to the beam direction were sorted against the detectors around 135° to produce a two-dimensional angular correlation matrix. To get clean DCO values for transitions in ^{79}Se, gates were usually set on uncontaminated stretched $E2$ transitions. In general, stretched quadrupole transitions were adopted if the DCO ratios were larger than 1.0, and stretched dipole transitions were assumed if DCO ratios were less than 0.8. The DCO ratio is plotted as a function of γ-ray energy for most of the observed transitions in ^{79}Se in Fig. 2.
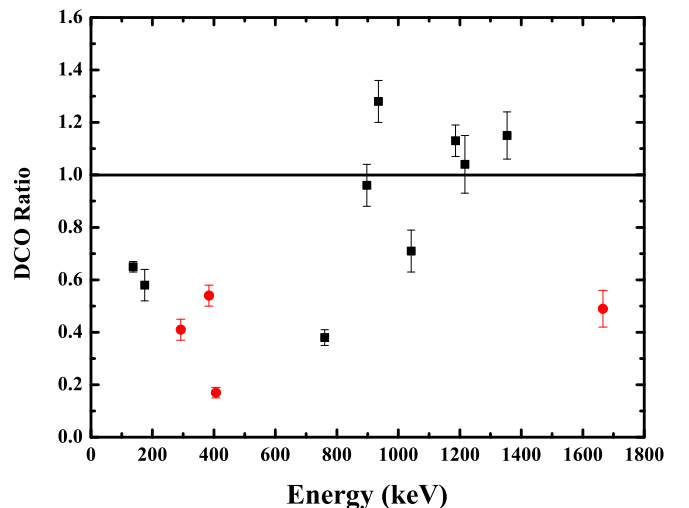

FIG. 2. The DCO ratio as a function of γ-ray energy for transitions in ^{79}Se. The transitions associated with band 2 are marked with circles; the other transitions are marked with squares.
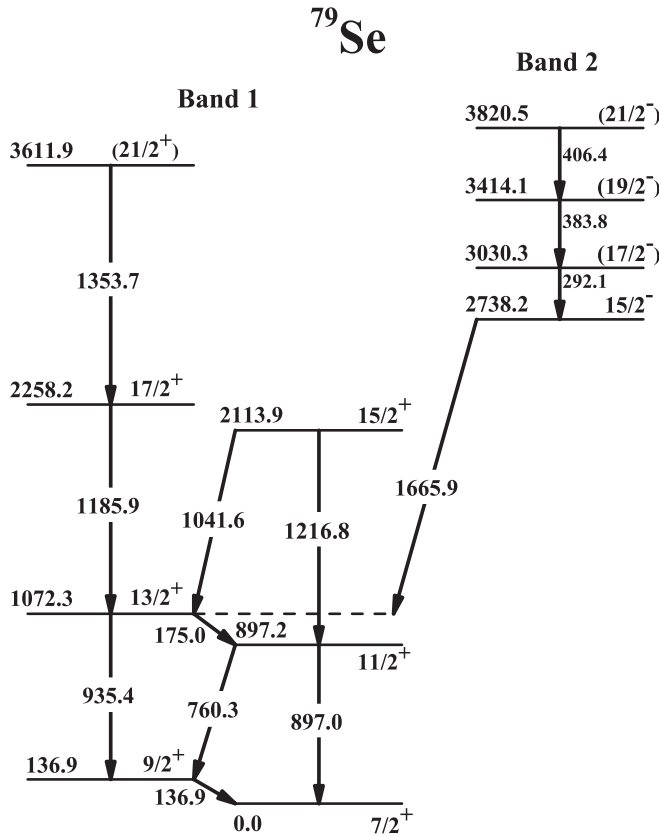
FIG. 3. Partial level scheme of ^{79}Se. Energies are in keV.

III. RESULTS AND DISCUSSION

The partial level scheme of ^{79}Se, deduced from the current work, is shown in Fig. 3, and agrees with those of previous works [22]. The $7/2^+$ ground state was suggested to have a $g_{9/2}$ configuration according to the measured nuclear moments [23], and the positive-parity band 1 was established up to spin $17/2^+$ at 2258.2 keV via the ^{76}Ge$(\alpha, n)^{79}$Se reaction

[22]. The present level scheme was constructed from $\gamma-\gamma$ coincidence relationships, intensity balances, and DCO ratios. The results are summarized in Table I. Although the $\Delta I = 2$ transitions for $19/2 \to 15/2$ (675.9 keV) and $21/2 \to 17/2$ (790.2 keV) in band 2 of ^{79}Se are not observed in the present work, the upper limits of the relative intensities of these two transitions are estimated with the analyses of the γ spectra.

For band 1, the level at 3611.9 keV was previously reported in Ref. [24], where no spin-parity was assigned to this level. According to the DCO value obtained in the current work, the transition of 1353.7 keV has a quadrupole transition character, implying that the level at 3611.9 keV has spin-parity $21/2^+$.

As shown in Fig. 3, in addition to the collective structure (band 1) built on the $g_{9/2}$ orbital, one new dipole band (band 2) is established in ^{79}Se. By requiring coincidence with the 136.9-keV transition of band 1, a cascade of 1665.9-, 292.1-, 383.8-, and 406.4-keV transitions is observed in Fig. 1. The 1665.9-keV transition was reported in Ref. [24] and a level at 2738.2 keV was placed without spin-parity assignment. The present DCO ratio analysis suggests stretched dipole natures for these γ-ray transitions. To distinguish the electric and magnetic character of the γ rays, linear polarization analyses [25] were performed by using the four clover detectors positioned at $90°$ relative to the beam direction as Compton polarimeters. The linear polarization value 0.57(21) suggests an $E1$ nature for the 1665.9-keV transition, whereas the linear polarization value $-0.40(32)$ suggests an $M1$ nature for the 383.8-keV transition. The 292.1- and 406.4-keV transitions for which the linear polarization values could not be extracted are most likely to be $M1$ transitions. This newly observed dipole band in ^{79}Se shares similar features of the three-quasiparticle bands in the $A \approx 80$ mass region summarized in Ref. [26]. In the neighboring isotope ^{77}Se [27] and isotone ^{81}Kr [28], the high-lying negative-parity dipole bands, which have a similar decay cascade in almost the same excitation energy range, were interpreted to have a three-quasiparticle configuration $\pi[(1g_{9/2})(fp)] \otimes \nu[(1g_{9/2})]$. The similarity of the dipole band in ^{79}Se to those in ^{77}Se and ^{81}Kr indicates

TABLE I. γ-ray energies, excitation energies, relative γ-ray intensities, DCO ratios, and spin-parity assignments in ^{79}Se.

E_γ (keV)	E_i (keV)	E_f (keV)	Intensity (%)	DCO ratio	Assignment
136.9	136.9	0.0	117.3(11)	0.65(2)	$9/2^+ \to 7/2^+$
175.0	1072.3	897.2	3.6(5)	0.58(6)	$13/2^+ \to 11/2^+$
292.1	3030.3	2738.2	7.0(8)	0.41(4)	$(17/2^-) \to 15/2^-$
383.8	3414.1	3030.3	6.2(8)	0.54(4)	$(19/2^-) \to (17/2^-)$
406.4	3820.5	3414.1	5.2(7)	0.17(2)	$(21/2^-) \to (19/2^-)$
675.9[a]	3414.1	2738.2	<1.0		$(19/2^-) \to (15/2^-)$
760.3	897.2	136.9	54.2(3)	0.38(3)	$11/2^+ \to 9/2^+$
790.2[a]	3820.5	3030.3	<2.1		$(21/2^-) \to (17/2^-)$
897.0	897.2	0.0	5.4(10)	0.96(8)	$11/2^+ \to 7/2^+$
935.4	1072.3	136.9	100	1.28(8)	$13/2^+ \to 9/2^+$
1041.6	2113.9	1072.3	11.2(15)	0.71(8)	$15/2^+ \to 13/2^+$
1185.9	2258.2	1072.3	45.5(33)	1.13(6)	$17/2^+ \to 13/2^+$
1216.8	2113.9	897.2	7.0(13)	1.04(11)	$15/2^+ \to 11/2^+$
1353.7	3611.9	2258.2	25.3(25)	1.15(9)	$(21/2^+) \to 17/2^+$
1665.9	2738.2	1072.3	5.5(13)	0.49(7)	$15/2^- \to 13/2^+$

[a]Not observed in the present work. The upper limit of relative intensity is estimated.
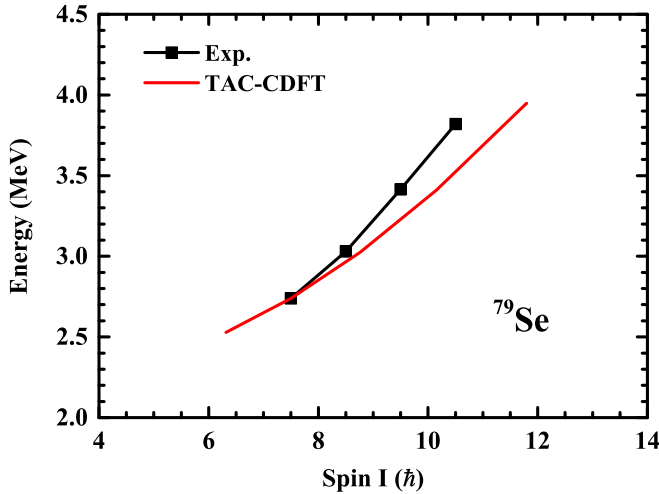
FIG. 4. The calculated energy spectrum obtained from the TAC-CDFT in comparison with the experimental data for band 2 in ^{79}Se.

that band 2 in ^{79}Se may also have the same three-quasiparticle configuration.

To further study the property of the dipole band (band 2) in ^{79}Se, especially its angular momentum forming mechanism, the TAC-CDFT [14] calculations with the PC-PK1 density functional [29] are performed. Based on the CDFT [30–33], which takes into account the Lorentz invariance, the TAC calculations have been successfully applied to describe many rotational phenomena, such as magnetic [34–37] and antimagnetic rotation [37–39], transition from collective to chiral rotation [40–42], and rotations with an exotic rod shape [43]. In particular, the TAC-CDFT calculation was performed for the high-lying dipole structure with configuration $\pi[(1g_{9/2})^1(1f_{5/2})^{-2}] \otimes \nu[(1g_{9/2})^5(fp)^{-3}]$ in ^{75}As [17], which has one fewer proton and three fewer neutrons than ^{79}Se. The dipole structure in ^{75}As is interpreted as a novel type of stapler band according to the TAC-CDFT results. In the present TAC-CDFT calculations, the same numerical details as for ^{75}As are used. The valence nucleon configuration adopted is $\pi[(1g_{9/2})^1(fp)^5] \otimes \nu[(1g_{9/2})^5]$, in correspondence to the assigned three-quasiparticle configuration at a rotational frequency of zero when neglecting pairing correlations.

In Fig. 4, the calculated energy spectrum as a function of spin by the TAC-CDFT is compared with the experimental data for band 2 in ^{79}Se. It can be seen that the calculated results reasonably reproduce the experimental excitation energies, which further supports the present configuration assignment for band 2. The slower increase for theoretical energy spectra at high spins suggests the overestimation of the moment of inertia, which can be attributed to the neglect of pairing correlations in the present calculations.

The theoretical reduced transition probabilities $B(M1)$ and $B(E2)$ for this dipole band are obtained with the TAC-CDFT calculations and presented in Table II. According to the calculations, its $B(E2)$ values are relatively small and the $B(M1)$ values are big, which is consistent with the experimental decay pattern (strong $\Delta I = 1$ transitions and nonobservable $\Delta I = 2$ transitions) of band 2 in ^{79}Se. When the spin

TABLE II. The calculated reduced transition probabilities $B(M1)$ and $B(E2)$ for the dipole band of ^{79}Se with TAC-CDFT.

$\hbar\omega$ (MeV)	Spin I ($\hbar$)	$B(M1)$ (μ_N^2)	$B(E2)$ (e^2b^2)
0.20	7.5	1.19	0.075
0.25	8.8	1.03	0.080
0.30	10.1	0.84	0.082
0.35	11.7	0.55	0.081

increases, the $B(M1)$ values decrease smoothly. Meanwhile, the $B(E2)$ values are relatively constant. Such a pattern is similar to that of magnetic dipole bands in ^{82,84}Rb [44,45]. The resulting theoretical $B(M1)/B(E2)$ ratios as a function of spin for the dipole band in ^{79}Se are plotted in Fig. 5 and compared with those in ^{75}As [17]. It can be seen that the trends of the $B(M1)/B(E2)$ ratio with spin for the dipole bands in ^{79}Se and ^{75}As are similar, while their slopes have a little difference. With the estimated upper limits of $\Delta I = 2$ transition intensities in the dipole band of ^{79}Se, the lower limits of the experimental $B(M1)/B(E2)$ ratios are obtained and presented in Fig. 5. It can be seen that the theoretical results are consistent with the experimental expectation.

In Fig. 6, the evolutions of deformation parameters β and γ with the rotational frequency for band 2 of ^{79}Se in the TAC-CDFT are presented, in comparison with those of the dipole band in ^{75}As [17]. In contrast to the relatively large triaxial deformation of the dipole band in ^{75}As, the dipole band of ^{79}Se has a relatively axially symmetric and small prolate deformation ($\beta \approx 0.22$ and $\gamma \approx 3°$).

To examine the angular momentum forming mechanism of the dipole band in ^{79}Se, the proton and neutron angular momentum vectors J_π and J_ν as well as the total angular momentum vector $J_{tot} = J_\pi + J_\nu$ at both the bandhead and the maximum rotational frequency obtained by the TAC-CDFT
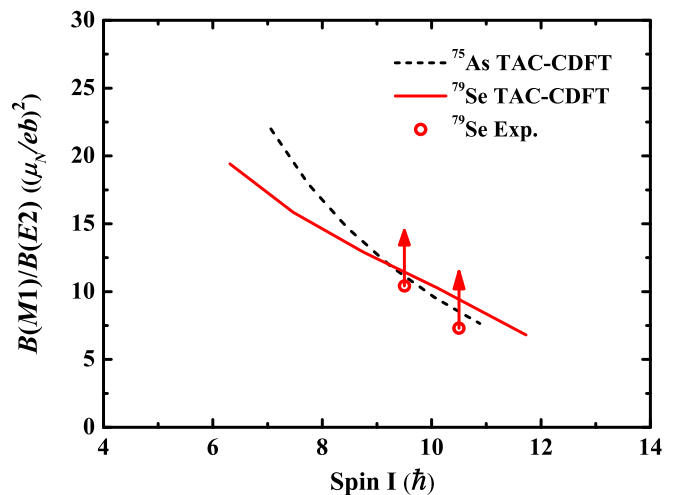

FIG. 5. The $B(M1)/B(E2)$ ratios for the stapler bands in ^{79}Se and ^{75}As as functions of the total angular momentum by the TAC-CDFT calculations in comparison with the deduced lower limits of experimental $B(M1)/B(E2)$ ratios of the stapler band in ^{79}Se from the present work.
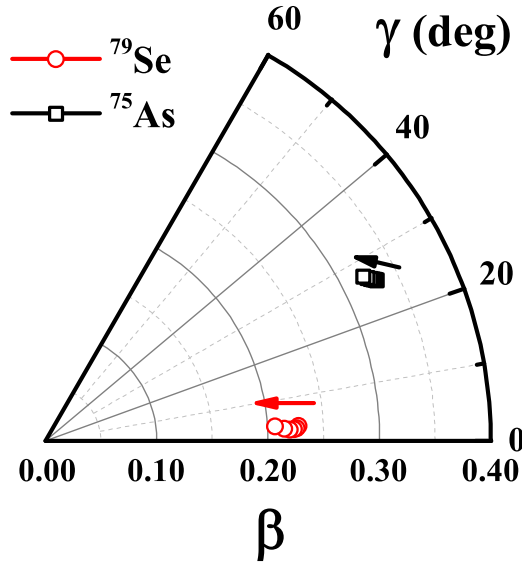
FIG. 6. Evolution of the deformation parameters β and γ driven by increasing rotational frequency in the TAC-CDFT calculations for the dipole bands in ^{79}Se and ^{75}As [17]. The arrows indicate the increasing direction of the rotational frequency $\hbar\omega$, which changes from 0.20 to 0.35 MeV in both cases.

calculations for band 2 are shown in Fig. 7(a), and the calculated results for the dipole band in ^{75}As are plotted in Fig. 7(b) for comparison. Here the proton and neutron angular momenta J_π and J_υ are the summation of the expectation values of the angular momentum over all the proton and neutron orbitals
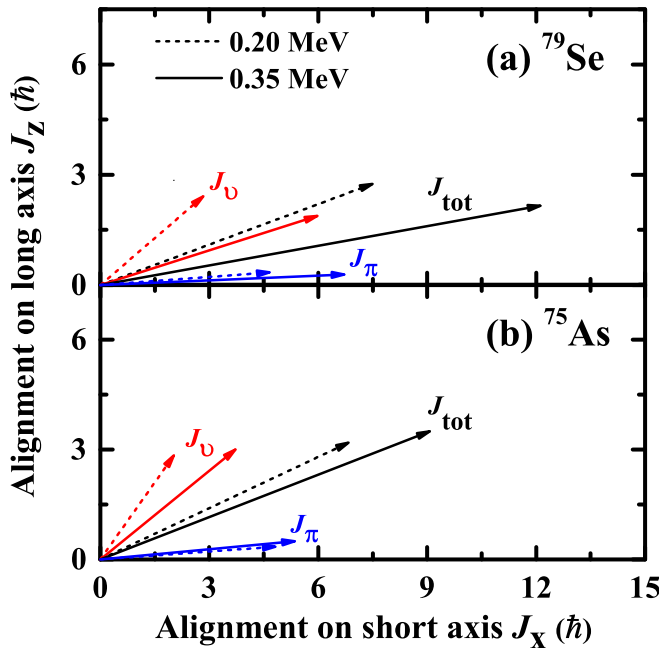

FIG. 7. Composition of the proton and neutron angular momentum vectors J_π and J_υ as well as the total angular momentum $J_{\text{tot}} = J_\pi + J_\upsilon$ at rotational frequencies $\hbar\omega = 0.20$ and 0.35 MeV in TAC-CDFT calculations for the dipole band in ^{79}Se, in comparison with that in ^{75}As [17].

occupied in the cranking wave function in the intrinsic system, respectively. In the TAC-CDFT calculations, both angular momentum components along the short and the long principal axes of nuclear density distribution can be obtained.

As shown in Fig. 7(a), for the dipole band in ^{79}Se, the protons mainly contribute the angular momentum along the x axis, whereas the neutrons contribute not only a large J_z component but also a substantial J_x component. With the increase of rotational frequency, only J_υ moves obviously toward the direction of the total angular momentum, whereas J_π only increases a little along the x axis. Consequently, the tilted angle of the total angular momentum has an obvious change. Although ^{75}As and ^{79}Se have different number parities in both proton number and neutron number, the angular momentum forming mechanism of the dipole band in ^{79}Se is similar to that of ^{75}As [cf. Fig. 7(b)]. Therefore, the dipole band in ^{79}Se can also be classified as a stapler band.

It is worth noting that although the J_z components of J_υ and J_π have almost similar behaviors in ^{75}As and ^{79}Se as a function of the frequency, the J_x components of J_υ and J_π in ^{79}Se increase faster than those of ^{75}As. As a result, the tilted angle of J_{tot} for ^{79}Se has a larger change than that of ^{75}As. At higher rotational frequency, it is found that J_{tot} of ^{79}Se totally aligns along the x axis at $\hbar\omega = 0.40$ MeV in the TAC-CDFT calculations, whereas J_{tot} of ^{75}As remains tilted even at $\hbar\omega = 0.45$ MeV [17]. The above differences can be understood as the dipole band in ^{79}Se has a nearly prolate shape which brings the collective rotation along the x axis, whereas the one in ^{75}As has a substantial triaxial deformation. Therefore, it is worth pointing out that the stapler bands can exist not only in oblate [16] and triaxial [17] nuclei, but also in prolate nuclei. Due to the effects of deformations, the stapler band is generated differently. For example, in the oblate case [16], it is mainly from the increase of the angular momentum component along the long axis. However, in the prolate case in ^{79}Se, it is mainly from the increase of the angular momentum component along the short axis.

To further illustrate the respective roles of the valence particles and core in the dipole band of ^{79}Se, the contributions to the total angular momentum from proton and neutron configurations in different shells as the rotational frequency increases from 0.20 to 0.35 MeV calculated with the TAC-CDFT are plotted in Fig. 8. Since there is no inert core in the TAC-CDFT calculations, the angular momentum increment coming from the $\pi[(1g_{9/2})^1(fp)^5]$ and $\upsilon[(1g_{9/2})^5]$ configurations is defined as the contribution of valence particles, while the core angular momentum is defined by the contribution from the rest of the nucleons, i.e., the 28 protons and the 40 neutrons.

As shown in Fig. 8, the angular momentum comes mainly from the contributions of the one proton and the five neutrons in the $1g_{9/2}$ orbitals, and slightly from the five protons in the f-p orbitals. The protons (neutrons) below the closed shells ($N = 40$, $Z = 28$) contribute little to the total angular momentum. For the neutrons, as the rotational frequency increases from 0.20 to 0.35 MeV, the contributions of the five neutrons in $1g_{9/2}$ orbitals increase significantly from $2.8\hbar$ to $6.0\hbar$ in the J_x component, whereas J_z has a slight decrease from $2.4\hbar$ to $1.9\hbar$. For the protons, the one proton in the $1g_{9/2}$ shell contributes a large component in J_x ($\approx 3.8\hbar$) and little in J_z
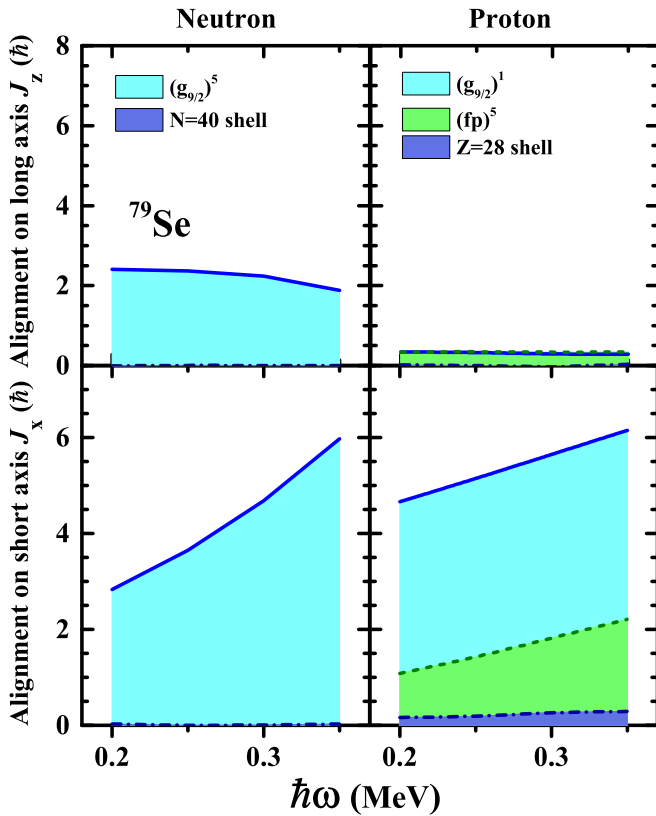
FIG. 8. The contributions to the total angular momentum from proton and neutron configurations in different shells as the rotational frequency increases from 0.20 to 0.35 MeV in the TAC-CDFT calculations.

(almost zero), but there are almost no increments of the J_x and J_z for this one proton as the frequency increases. The five protons in the *f-p* shell contribute to a gradual increase in the J_x component from $0.9\hbar$ to $1.9\hbar$ as the frequency increases from 0.20 to 0.35 MeV, whereas the J_z component remains constant ($\approx 0.3\hbar$). The protons below the $Z = 28$ closed shell contribute very little. There are only about $0.2\hbar$ contribution to the J_x component and almost no contribution to the J_z component.

This angular momentum coupling indicates that for the dipole band in ^{79}Se, the valence nucleons in the high-j orbitals play a major role in the increase of the angular momentum which is similar to ^{75}As [17]. For the dipole bands in ^{79}Se

and ^{75}As, there is an obvious difference in their deformations as clearly seen in Fig. 6. Similar stapler mechanisms are therefore ascribed to their high-j valence nucleons: the five neutrons in the $1g_{9/2}$ orbital and the one proton in the $1g_{9/2}$ orbital, although the two nuclei have different number parities in both proton number and neutron number.

IV. SUMMARY

The spectroscopy of ^{79}Se was studied via the ^{82}Se$(\alpha, \alpha3n)^{79}$Se fusion-evaporation reaction at beam energies of 65 and 68 MeV. A negative-parity magnetic dipole band was newly observed. The properties of the dipole band in ^{79}Se were investigated in terms of the TAC-CDFT with the configuration $\pi[(1g_{9/2})^1(fp)^5] \otimes \upsilon[(1g_{9/2})^5]$. The calculated energy spectrum reasonably reproduces the experimental excitation energies. The TAC-CDFT calculations indicate that this dipole band has a relatively stable symmetric prolate deformation as a function of the rotational frequency. Based on the angular momentum forming mechanism, the dipole band in ^{79}Se can be classified as a stapler band, where the five valence nucleons in the $1g_{9/2}$ orbital are responsible for the closing of the stapler of the angular momentum. It shares a similar stapler mechanism with ^{75}As. It is noted that only the lower limits of the experimental $B(M1)/B(E2)$ ratios for the dipole band in ^{79}Se are obtained in the present experiment. To further justify its stapler mechanism, more experimental studies, especially lifetime measurement, are still necessary.

[1] E. Teller and J. A. Wheeler, Phys. Rev. **53**, 778 (1938).

[2] A. Bohr and B. R. Mottelson, *Nuclear Structure* (Benjamin, New York, 1975), Vol. II.

[3] A. Bohr, Phys. Rev. **81**, 134 (1951).

[4] A. Johnson, H. Ryde, and J. Sztarkier, Phys. Lett. B **34**, 605 (1971).

[5] P. J. Twin, B. M. Nyakó, A. H. Nelson, J. Simpson, M. A. Bentley, H. W. Cranmer-Gordon, P. D. Forsyth, D. Howe, A. R. Mokhtar, J. D. Morrison, J. F. Sharpey-Schafer, and G. Sletten, Phys. Rev. Lett. **57**, 811 (1986).

[6] S. Frauendorf and J. Meng, Nucl. Phys. A **617**, 131 (1997).

[7] S. Y. Wang, B. Qi, L. Liu, S. Q. Zhang, H. Hua, X. Q. Li, Y. Y. Chen, L. H. Zhu, J. Meng, S. M. Wyngaardt, P. Papka, T. T. Ibrahim, R. A. Bark, P. Datta, E. A. Lawrie, J. J. Lawrie, S. N. T. Majola, P. L. Masiteng, S. M. Mullins, J. Gál, G. Kalinka, J. Molnár, B. M. Nyakó, J. Timár, K. Juhász, and R. Schwengnerand, Phys. Lett. B **703**, 40 (2011).

[8] C. Liu, S. Y. Wang, R. A. Bark, S. Q. Zhang, J. Meng, B. Qi, P. Jones, S. M. Wyngaardt, J. Zhao, C. Xu, S. G. Zhou, S. Wang, D. P. Sun, L. Liu, Z. Q. Li, N. B. Zhang, H. Jia, X. Q. Li, H.

Hua, Q. B. Chen, Z. G. Xiao, H. J. Li, L. H. Zhu, T. D. Bucher, T. Dinoko, J. Easton, K. Juhász, A. Kamblawe, E. Khaleel, N. Khumalo, E. A. Lawrie, J. J. Lawrie, S. N. T. Majola, S. M. Mullins, S. Murray, J. Ndayishimye, D. Negi, S. P. Noncolela, S. S. Ntshangase, B. M. Nyakó, J. N. Orce, P. Papka, J. F. Sharpey-Schafer, O. Shirinda, P. Sithole, M. A. Stankiewicz, and M. Wiedeking, Phys. Rev. Lett. **116**, 112501 (2016).

[9] S. Frauendorf, J. Meng, and J. Reif, in *Proceedings of the Conference on Physics from Large γ-Ray Detector Arrays*, edited by M. A. Deleplanque (University of California, Berkeley, CA, 1994), Vol. II, p. 52.

[10] S. Frauendorf, Z. Phys. A **358**, 163 (1997).

[11] R. M. Clark and A. O. Macchiavelli, Annu. Rev. Nucl. Part. Sci. **50**, 1 (2000).

[12] S. Frauendorf, Rev. Mod. Phys. **73**, 463 (2001).

[13] H. Hübel, Prog. Part. Nucl. Phys. **54**, 1 (2005).

[14] J. Meng, J. Peng, S. Q. Zhang, and P. W. Zhao, Front. Phys. **8**, 55 (2013).

[15] S. Frauendorf, Nucl. Phys. A **557**, 259 (1993).

[16] Z. Q. Chen, S. Y. Wang, L. Liu, P. Zhang, H. Jia, B. Qi, S. Wang, D. P. Sun, C. Liu, Z. Q. Li, X. G. Wu, G. S. Li, C. Y. He, Y. Zheng, and L. H. Zhu, Phys. Rev. C **91**, 044303 (2015).

[17] C. G. Li, Q. B. Chen, S. Q. Zhang, C. Xu, H. Hua, X. Q. Li, X. G. Wu, S. P. Hu, J. Meng, F. R. Xu, W. Y. Liang, Z. H. Li, Y. L. Ye, D. X. Jiang, J. J. Sun, R. Han, C. Y. Niu, X. C. Chen, P. J. Li, C. G. Wang, H. Y. Wu, G. S. Li, C. Y. He, Y. Zheng, C. B. Li, Q. M. Chen, J. Zhong, and W. K. Zhou, Phys. Lett. B **766**, 107 (2017).

[18] J. Peng and W. Q. Xu, Chin. Phys. Lett. **33**, 012101 (2016).

[19] Y. Y. Cheng, S. Q. Zhang, X. Q. Li, H. Hua, C. Xu, Z. H. Li, P. W. Zhao, J. Meng, J. J. Sun, Z. J. Bai, F. R. Xu, Y. L. Ye, D. X. Jiang, E. H. Wang, C. He, R. Han, X. G. Wu, G. S. Li, C. Y. He, Y. Zheng, C. B. Li, S. P. Hu, S. H. Yao, B. B. Yu, X. P. Cao, and J. L. Wang, Phys. Rev. C **89**, 054309 (2014).

[20] J. F. Sharpey-Schafer, Nucl. Phys. News **14**, 5 (2004).

[21] D. C. Radford, Nucl. Instrum. Methods Phys. Res. Sect A **361**, 297 (2005).

[22] B. Singh, Nucl. Data Sheets **135**, 193 (2016).

[23] W. A. Hardy, G. Silvey, C. H. Townes, B. F. Burke, M. W. P. Strandberg, G. W. Parker, and V. W. Cohen, Phys. Rev. **92**, 1532 (1953).

[24] L. Funke, J. Döring, R. Schwengner, and G. Winter, Report No. ZFK-621, 1987, p. 35.

[25] P. M. Jones, L. Wei, F. A. Beck, P. A. Butler, T. Byrski, G. Duchêne, G. de France, F. Hannachi, G. D. Jones, and B. Kharraja, Nucl. Instrum. Methods Phys. Res. Sect A **362**, 556 (1995).

[26] S. L. Tabor and J. Döring, Phys. Scr. **T56**, 175 (1995).

[27] G. D. Johns, J. Döring, R. A. Kaye, G. N. Sylvan, and S. L. Tabor, Phys. Rev. C **55**, 660 (1997).

[28] L. Funke, J. Döring, P. Kemnitz, E. Will, G. Winter, A. Johnson, L. Hildingsson, and T. Lindblad, Nucl. Phys. A **455**, 206 (1986).

[29] P. W. Zhao, Z. P. Li, J. M. Yao, and J. Meng, Phys. Rev. C **82**, 054319 (2010).

[30] P. Ring, Prog. Part. Nucl. Phys. **37**, 193 (1996).

[31] D. Vretenar, A. V. Afanasjev, G. A. Lalazissis, and P. Ring, Phys. Rep. **409**, 101 (2005).

[32] J. Meng, H. Toki, S. G. Zhou, S. Q. Zhang, W. H. Long, and L. S. Geng, Part. Nucl. Phys. **57**, 470 (2006).

[33] *Relativistic Density Functional for Nuclear Structure*, International Review of Nuclear Physics Vol. 10, edited by J. Meng (World Scientific, Singapore, 2016).

[34] J. Peng, J. Meng, P. Ring, and S. Q. Zhang, Phys. Rev. C **78**, 024313 (2008).

[35] P. W. Zhao, S. Q. Zhang, J. Peng, H. Z. Liang, P. Ring, and J. Meng, Phys. Lett. B **699**, 181 (2011).

[36] L. F. Yu, P. W. Zhao, S. Q. Zhang, P. Ring, and J. Meng, Phys. Rev. C **85**, 024318 (2012).

[37] J. Peng and P. W. Zhao, Phys. Rev. C **91**, 044329 (2015).

[38] P. W. Zhao, J. Peng, H. Z. Liang, P. Ring, and J. Meng, Phys. Rev. Lett. **107**, 122501 (2011).

[39] P. W. Zhao, J. Peng, H. Z. Liang, P. Ring, and J. Meng, Phys. Rev. C **85**, 054310 (2012).

[40] P. W. Zhao, S. Q. Zhang, and J. Meng, Phys. Rev. C **92**, 034319 (2015).

[41] P. W. Zhao, Phys. Lett. B **773**, 1 (2017).

[42] P. W. Zhao, Y. K. Wang, and Q. B. Chen, Phys. Rev. C **99**, 054319 (2019).

[43] P. W. Zhao, N. Itagaki, and J. Meng, Phys. Rev. Lett. **115**, 022501 (2015).

[44] H. Schnare, R. Schwengner, S. Frauendorf, F. Dönau, L. Käubler, H. Prade, A. Jungclaus, K. P. Lieb, C. Lingk, S. Skoda, J. Eberth, G. de Angelis, A. Gadea, E. Farnea, D. R. Napoli, C. A. Ur, and G. Lo Bianco, Phys. Rev. Lett. **82**, 4408 (1999).

[45] H. Madokoro, J. Meng, M. Matsuzaki, and S. Yamaji, Phys. Rev. C **62**, 061301(R) (2000).